Imaging Focal Sites of Bacterial Infection in Rats with Indium-111-Labeled Chemotactic Peptide Analogs

Alan J. Fischman, Marilyn C. Pike, Daniel Kroon, Anthony J. Fucello, Douglas Rexinger, Caroline tenKate, Robert Wilkinson, Robert H. Rubin, and H. William Strauss

Nuclear Medicine Division, Department of Radiology and the Infectious Disease and Arthritis Units of the Medical Service, Massachusetts General Hospital, Boston, Massachusetts, Departments of Radiology and Medicine, Harvard Medical School, Boston, Massachusetts, and the R.W. Johnson Pharmaceutical Research Institute, Raritan, New Jersey

Four DTPA-derivatized chemotactic peptide analogs: ForNleLFNleYK-DTPA (P1), ForMLFNH(CH_2)$_6$NH-DTPA (P2), ForNleLFK(NH2)-DTPA (P3), and ForNleLFK-DTPA (P4), were synthesized and evaluated for in vitro bioactivity and receptor binding. The peptides were radiolabeled with ^{111}In by transchelation and their biodistribution determined in rats at 5, 30, 60 and 120 min after injection. Localization at sites of infection was determined by scintillation camera imaging in animals with deep-thigh infection due to *Escherichia coli*. Images were recorded from 5 min to 2 hr after injection. All peptides maintained biologic activity (EC_{50} for O_2^- production by human PMN's: 3-150 n*M*) and the ability to bind to the oligopeptide chemoattractant receptor on human PMN's (EC_{50} for binding: 7.5–50 n*M*); biologic activity and receptor binding were highly correlated ($r = 0.99$). For all the peptides, blood clearance was rapid (half-lives: 21.5, 33.1, 31.6, and 28.7 min for P1, P2, P3, and P4, respectively). Biodistributions of the individual peptides were similar with low levels of accumulation in the heart, lung, liver, spleen, and gastrointestinal tract. In the kidney, P1 had much greater accumulation than other organs. All peptides yielded high quality images of the infection sites within 1 hr of injection. This study demonstrates that ^{111}In-labeled chemotactic peptide analogs were effective agents for the external imaging of focal sites of infection.

J Nucl Med 1991; 32:483–491

Treatment of the patient with suspected infection requires prompt identification of the site and extent of the process. Imaging with gallium-67- (^{67}Ga)-citrate (*1*), indium-111- (^{111}In)-labeled white blood cells (*2*), or ^{111}In-labeled IgG (*3,4*) can localize infections, but usually requires 12–24 hr before lesions can be visualized. This represents a serious deficiency in the radionuclide approaches, compared to ultrasound or computed tomography, where lesions are usually apparent at the conclusion of the imaging procedure. The explanation for the lengthy time required for infection localization with ^{67}Ga-citrate and ^{111}In-labeled IgG is related in part to the high molecular weight of the species taken up by the lesion. IgG has a molecular weight of approximately 150 kDa. In the case of gallium, the radionuclide circulates bound to transferrin or lactoferrin (molecular weights ~ 100 kDa) (*5*). While inflammatory lesions usually have increased vascular permeability, the diffusion barrier to molecules of this size range is still substantial, resulting in slow delivery of the radiopharmaceutical to the lesion. In addition, since blood clearance of these molecules takes place over many hours, background activity remains high, resulting in a low target-to-background ratio in the early hours after injection. The situation with ^{111}In-labeled white blood cells is different. The radiolabeled cells require several hours to localize after injection because they must detect the chemoattractant signal before migrating to the site of inflammation.

The interval between injection and lesion detection could be substantially reduced by the availability of a small molecule capable of binding to circulating granulocytes as well as to leukocytes already present at the time of inflammation. Among the candidate molecules for this task, certain leukocyte chemattractant peptides looked particularly promising. The parent compound of this group, N-formyl-methionyl-leucyl-phenylalanine (MW 437), is a bacterial product that is known to initiate leukocyte chemotaxis by binding to high affinity receptors on the white blood cell membrane (*6–8*). These receptors are present on polymorphonuclear neutrophils (PMNs) and mononuclear phagocytes. As granulocytes respond to the chemoattractant gradient, the affinity of the receptors decreases as additional receptors are expressed, until the granulocyte reaches the site of inflammation, where the concentration of chemoattrac-

Received July 27, 1990; revision accepted Oct. 1, 1990.
For reprints contact: Alan J. Fischman, MD, PhD, Division of Nuclear Medicine, Massachusetts General Hospital, Fruit St., Boston MA 02114.

tant is greatest (*9–11*). Based on this information, we hypothesized that radiolabeled chemoattractant peptides should localize rapidly at focal sites of inflammation.

Previous studies demonstrated that many synthetic analogs of these small, N-formyl-methionyl peptides bind to neutrophils and macrophages with equal or greater affinity compared to the native peptide (*6,11, 12*). In the present work, we report the synthesis of a series of analogs of these peptides that can be readily labeled with ^{111}In. These reagents were tested both in vitro and in vivo. The in vitro studies evaluated their ability to bind to neutrophil receptors and induce the production of superoxide; while the in vivo evaluation determined their biodistribution in healthy animals, the changes in peripheral white blood count as a result of intravenous administration of one agent and their localization at focal sites of inflammation.

MATERIALS AND METHODS

Materials

N-formyl-methionyl-leucyl-phenylalanine (ForMLF), N-formyl-norleucyl-leucyl-phenylalanyl-norleucyl-tyrosyl-lysine (ForNleLPNLeYK), phorbol myristate acetate (PMA), and cytochalasin B were obtained from Sigma (St. Louis, MO). ForML[^{3}H]F (60 Ci/mmol) was obtained from New England Nuclear (Boston, MA) and ^{111}In-chloride from Amersham (Arlington Heights, IL). Hanks' balanced salt solution (HBSS) was obtained from Gibco (Grand Island, NY).

Peptide Synthesis and Characterization

For-NleLFNleYK-DTPA (P1), and For-NleLFK-DTPA (P4) were synthesized by the Merrifield solid-phase technique (*13*) as detailed by Stewart and Young (*14*). Briefly, t-butyloxycarbonyl (Boc) protected amino acids were added sequentially to a Lys(2-chlorobenzyloxycarbonyl) resin ester which was prepared from chloromethyl resin by the method of Gisin (*15*). After removal of the amino terminal Boc group, the peptides were formylated with formic-acetic anhydride by the method of Sheehan and Yang (*16*). The peptides were cleaved from the resin with anhydrous liquid hydrogen fluoride (HF) containing 10% p-cresol (added as a scavenger for free radicals) at 0°C for 1 hr. The crude peptides (~100 mg, P1: 0.12 mmol, P4: 0.18 mmol) were dissolved in DMF along with diisopropylethylamine (0.24 mmol) and the mixture was added in small portions over 30 min to a slurry of diethylenetriaminepentaacetic acid (DTPA) dianhydride (0.36 mmol) in a small volume of DMF. After an additional hour of stirring, water was added to hydrolyze remaining anhydride. The solvent was removed by rotary evaporation and water was added to the residue. The precipitate was filtered and washed with water. A mixture of the monomeric and dimeric conjugate of DTPA was obtained, which could be separated by chromatography. The peptides were dissolved in 0.10 *M* ammonium bicarbonate and purified by ion-exchange chromatography on a mono-Q FPLC column eluted with a gradient of 0.10–0.50 *M* ammonium bicarbonate, pH 8. The fractions containing the major product were lyophilized.

For-MLFNH$(CH_2)_6$NH-DTPA (P2) was synthesized in a similar fashion on an oxime resin (*17*), starting with the coupling of Boc-Phe to the resin. After sequential addition of Boc-Leu and Boc-Met and formylation, the resin was treated with 1.5% hexanediamine in DMF for 4 hr, which cleaved the peptide from the resin as the hexanediamine derivative. The product was isolated by washing the resin with DMF and evaporating the DMF and precipitation with ether. The peptide was conjugated with DTPA by the procedure described above. The product was purified by high-performance liquid chromatography (HPLC) on a Whatman Partisil 10 ODS-3 column eluted with a gradient of 30%–50% acetonitrile in 0.1% trifluoroacetic acid (TFA). The peptide was isolated by stripping acetonitrile on a rotary evaporator followed by lyophilization.

For-NleLFK(NH_2)-DTPA (P3) was similarly prepared by solid-phase peptide synthesis with p-methylbenzhydylamine resin. After reaction with DTPA anhydride, the peptide-DTPA conjugate was purified by preparative HPLC with an acetonitrile/0.1% FTA gradient.

The purity of the peptides was assessed by analytical reversed-phase HPLC. Mass spectra and amino acid analysis agreed with the expected values.

Cell Preparation

Human peripheral blood PMNs were isolated by sedimentation in 3% Dextran (Pharmacia, Nutley, NJ) followed by gradient centrifugation on Lymphoprep (Organon Teknika, Durham, NC) as previously described (*8,18*). Cell preparations contained >95% polymorphonuclear leukocytes (PMNs) as assessed by light microscopy of Wright-stained specimens.

ForML[^{3}H]F Receptor Binding Assay

Isolated human PMNs (obtained from healthy volunteers), 8×10^5, were incubated in phosphate-buffered saline containing 1.7 mM KH_2PO_4, 8.0 m*M* Na_2HPO_4, 0.117 *M* NaCl, 0.15 m*M* $CaCl_2$, 0.5 m*M* $MgCl_2$, and 1.0 m*M* PMSF pH 7.4 (incubation buffer) at 24°C for 45 min in a total volume of 0.15 ml in the presence and absence of the indicated concentration of derivatized peptide and 15 n*M* Formyl [^{3}H]F (*6, 19*). Following incubation, the cells were filtered onto glass fiber discs (Whatman GF/C; Whatman, Inc., Clifton, NJ), which were then washed with 20 ml of ice cold incubation buffer. The filters were placed in scintillation vials with 10 ml of Safety-Solve (Research Products International Corp., Mt. Prospect, IL) and the radioactivity was measured by liquid scintillation spectroscopy. Specific binding is defined as total binding minus nonspecific binding, which is the amount of residual radioactivity bound in the presence of 10 μM unlabeled ForMLF (*19*). Nonspecific binding was approximately 10% of total binding.

Assay of Superoxide Production

Superoxide release by human neutrophils was assayed by monitoring the superoxide dismutase-inhibitable reduction of ferricytochrome C using an extinction coefficient of 29.5 mmol/l/cm as previously described (*20*). Briefly, isolated human cells were incubated with HBSS alone or with increasing concentrations of the four peptide analogs, ForMLF or ForNleLPNleYK ranging from 1 n*M* to 1 u*M* in the presence of 10 μM cytochalasin B plus or minus superoxide dismutase

(50 μg/ml) at 37°C for 10 min, after which the reduction of ferricytochrome C was measured spectrophotometrically.

Indium-111 Labeling

The chemotactic peptide analogs were radiolabeled with ^{111}In by transchelation. Briefly, a 5-μl aliquot of a stock solution of peptide (1.0 mg/ml in DMSO) was diluted with 0.5 ml of 1.0 *M* citrate buffer (pH 5.0) and combined with 1–2 mCi of ^{111}In-Cl_3 immediately prior to use. The mixture was incubated for 30 min at room temperature, applied to a column of Sephadex G-10, and the peptide fraction isolated. The pooled fractions were passed through a 0.22-micron filter (Millipore Corp., Bedford, MA) prior to injection. Chemical purity of the labeled products were determined by HPLC as described above. Optical density was monitored at 280 nm and fractions were collected and radioactivity measured with a well-type gamma scintillation counter (LKB model 1282, Wallac Oy, Finland).

In-Vivo Studies

Three studies were performed in animals:

1. To determine the effect of peptide on circulating granulocytes, unlabeled peptides were administered to anesthetized rats at doses planned for imaging and serial white cell counts were performed.
2. To define the in-vivo distribution of the radiolabeled peptide analogs in healthy animals, biodistribution studies were performed with each analog.
3. The ability of radiolabeled peptide analogs to localize at focal sites of inflammation was determined from serial gamma camera images recorded in animals with *Escherichia coli* infection.

Effect of a Chemotactic Peptide Analog on Peripheral WBC Levels in Rats. Adult male Sprague-Dawley rats were lightly restrained and a baseline blood sample (0.2 ml) was drawn from the tail vein into heparinized syringes. The animals were then injected with 1 nmole of P1 via the tail vein. At 5, 10, 20, and 40 min after injection, additional blood samples were obtained. All blood samples were stored on ice until the conclusion of the experiment at which time total white counts were determined with a hemocytometer.

Biodistribution. Groups of thirty uninfected rats were injected with about 10 μCi of peptide labeled with ^{111}In to determine the biodistribution at 5, 10, 30, 60, and 120 min (each peptide was evaluated in six animals at each time point). Samples of blood, lung, liver, spleen, kidney, muscle, and intestine were weighed and counted in a well-type gamma counter (LKB model 1282, Wallac Oy, Finland). In other groups of rats receiving ^{111}In-P1, cells were separated from plasma and the amount of cell associated radioactivity was determined. To correct for radioactive decay and permit calculation of activity in each organ as a fraction of the administered dose, aliquots of the injected doses were counted simultaneously. The results were expressed as percent injected dose per gram (%ID/g) (*21*).

Studies in Infected Animals. A single clinical isolate of *Escherichia coli* was employed to produce focal infection. The bacteria were incubated overnight on trypticase soy agar plates at 37°C, and individual colonies were diluted with sterile normal saline to produce a turbid suspension containing approximately 2×10^9 organisms/ml. Male Sprague-Dawley rats, weighing approximately 200 g (Charles River Breeding Laboratories, Burlington, MA) were anesthetized with ketamine and injected in their left posterior thigh with 0.1 ml of a suspension containing approximately 2×10^8 organisms.

Twenty-four hours after bacterial inoculation, when gross swelling was apparent in the thigh, one of the radiolabeled peptides (~0.25 mg/kg labeled with 100–150 μCi of ^{111}In) was injected intravenously via the tail vein. The animals were anesthetized with ketamine and serial whole-body scintigrams were acquired using a large field of view scintillation camera equipped with a parallel-hole medium-energy collimator interfaced to a dedicated computer system (Technicare 438, Technicare 560, Solon, Ohio). Images were recorded for a preset time of 5 min/view with a window centered to include both the 173 and 247 keV photopeaks of ^{111}In.

Regions of interest were drawn around the infected area, a similar area in the contralateral thigh, and the whole animal to calculate target-to-background (T/B) ratios (infected thigh/contralateral thigh) and percent residual activity (%RA) (infected thigh/whole animal). At the conclusion of imaging, the animals were killed with ether anesthesia and autopsied to evaluate the infection. Cultures of the site of infection were obtained at this time.

Statistical Methods

The results of the imaging and biodistribution studies were evaluated by analysis of variance followed by Duncan's new multiple range test (*22*). All results are expressed as mean ± s.e.m.

RESULTS

Peptide Synthesis

All four DTPA-derivatized chemotactic peptide analogs were prepared in good yield and purity. While a significant amount of dimer formation occurred by using the bicyclic anhydride of DTPA for introducing the metal chelation site, the two forms were readily separated by ion-exchange chromatography as demonstrated by mass spectroscopy of the final products.

Biologic Activity of Chemotactic Peptide Analogs

Figure 1 shows that peptides P1, P2, and P4 produced superoxide with potencies similar to the underivatized hexapeptide, ForNleLFNleYK. The concentrations of peptides that produced 50% of a maximal response (EC_{50}) were 9 n*M*, 12 n*M*, 3 n*M*, and 15 n*M* for ForNleLFNleYK, P1, P2, and P4, respectively. Peptide P3 was less potent than the other peptide analogs with an EC_{50} of 150 n*M*, which is similar to ForMLF (EC_{50} = 60 n*M*).

The efficacy of the peptides, defined as the maximal amount of superoxide anion produced, was similar for all peptides tested and ranged between 13.3 and 16.3 nmole O_2^- produced/10^6 cells/10 min. The efficacy of all the peptides was less than that for phorbol myristate acetate (PMA), an unrelated activator of the PMN

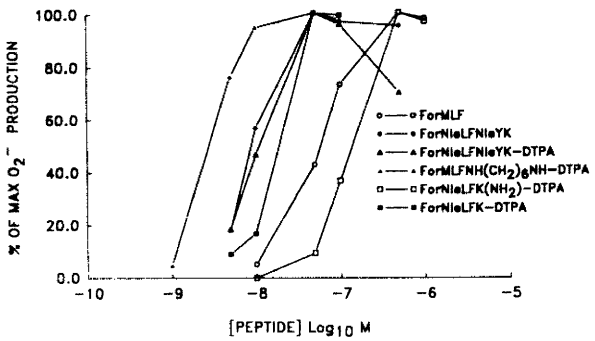

FIGURE 1
Superoxide production by chemotactic peptide analogs. Human PMNs were incubated with HBSS alone or the indicated concentration of peptide for 10 min at 37°C, after which the reduction of ferricytochrome was measured as described in the text.

% of maximal superoxide production = E/M × 100,

where E is the amount of superoxide produced in the presence of an indicated concentration of peptide and M is the maximal amount of O_2^- produced by the peptide. ForNleLFNleYK-DTPA: P1, ForMLFNH$(CH_2)_6$NH-DTPA: P2, ForNleLFK(NH2)-DTPA: P3, ForNleLFK-DTPA: P4.

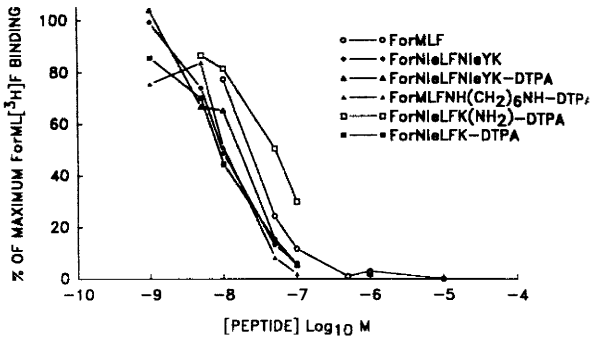

FIGURE 2
Effect of chemotactic peptide analogs on ForML[^{3}H]F binding to human PMNs. Intact Human PMNs (8×10^5) were incubated with incubation buffer or the indicated concentration of peptide in the presence of 15 n*M* ForML[^{3}H]F for 45 min at 24°C, after which the specific ForML[^{3}H]F binding was determined.

% of maximal ForML[^{3}H]F binding = E/C × 100,

where E is the specific CPM bound in the presence of the indicated concentration of unlabeled peptide and C is the specific CPM bound of ForML[^{3}H]F in the presence of buffer alone. ForNleLFNleYK-DTPA: P1, ForMLFNH$(CH_2)_6$NH-DTPA: P2, ForNleLFK(NH2)-DTPA: P3, ForNleLFK-DTPA: P4.

oxidative burst, which gave a maximal response of 22.9 nmole O_2^- produced/10^6 cells/10 min at a concentration of 0.1 μM.

Interaction of Chemotactic Peptide Analogs with the N-Formyl Peptide Chemoattractant Receptor on Human Leukocytes

Figure 2 shows that the chemotactic peptide analogs compete for the binding of ForML[^{3}H]F to intact human PMNs with an order of potency similar to that noted for production of superoxide anion. The EC_{50}'s for inhibition of ForML[^{3}H]F binding of peptides P1, P2, P4, and ForNleLFNleYK were very similar; ranging from 7.5 to 10 n*M*. Peptide P3 was the least potent with an EC_{50} of 50 n*M* for inhibition of ForML[^{3}H]F binding and ForMLF was intermediate with an EC_{50} of 25 n*M*. Thus, the orders of potency for production of superoxide anion and inhibition of ForML[^{3}H]F binding were very similar; peptides P1, P2, and P4 were approximately equal to ForNleLFNleYK and ForMLF, while peptide P3 was substantially less potent. Regression analysis of the EC_{50} for receptor binding vs the EC_{50} for superoxide production was readily fit by a linear model (R = 0.995) (Fig. 3).

Effect of a Chemotactic Peptide Analog on Peripheral PMN Levels

The time course of the effect of i.v. injection of 1.0 nmole of P1 on peripheral WBC levels in rats illustrated in Figure 4. Significant variation in baseline WBC levels between rats was observed; however, the overall effect of peptide injection was modest. Analysis of variance demonstrated a significant main effect of time after injection on WBC level, $F_{4,25} = 6.18$; $p < 0.005$. Levels at 40 min postinjection were significantly lower than at baseline, 5 min, and 10 min ($p < 0.01$), and levels at 20 min were significantly lower than at 5 min and 10 min ($p < 0.05$).

Indium-111 Labeling

Figure 5 illustrates the behavior of ^{111}In-P1 on HPLC. As can be seen, a single major peak was detected by both ultraviolet absorbance (OD_{280}) and radioactivity detection. In the radioactivity tracing, a minor peak representing < 5% of total radioactivity was also detected. Similar results were obtained with the other three ^{111}In-labeled peptides.

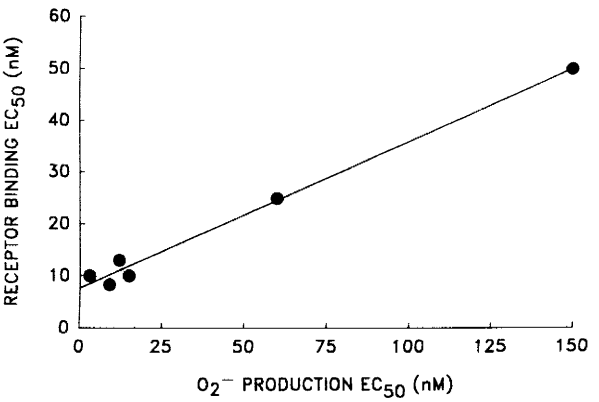

FIGURE 3
Regression analysis of the EC_{50} for receptor binding versus EC_{50} for superoxide production. A linear model yielded an excellent fit to the data (r = 0.995, slope = 0.283, and intercept = 7.66).

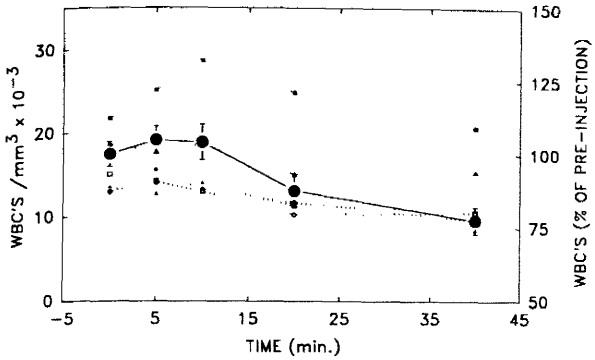

FIGURE 4
Effect of P1 on peripheral WBC levels in rats. Animals were injected with peptide and WBC levels determined as described in the text. Dotted lines indicate WBC levels in individual rats and the solid line indicates percent of preinjection baseline levels.

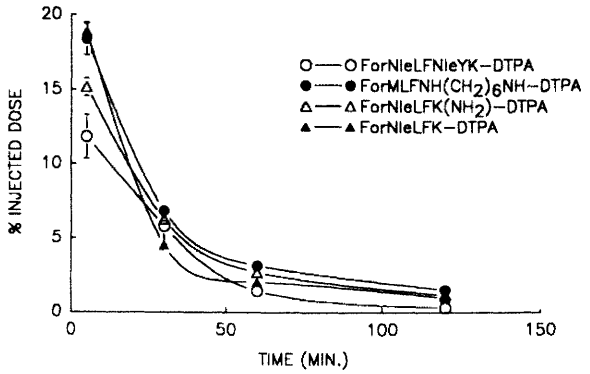

FIGURE 6
Blood clearance of ^{111}In-labeled chemotactic peptide analogs in uninfected rats. Data are presented as percent total activity. Each point is the mean ± s.e.m. for six animals. ForNleLFNleYK-DTPA: P1, ForMLFNH(CH$_2$)$_6$NH-DTPA: P2, ForNleLFK(NH2)-DTPA: P3, ForNleLFK-DTPA: P4.

Biodistribution

All four DTPA-derivatized chemotactic peptide analogs showed a similar monotonic decrease in blood activity over time (Fig. 6). Analysis of variance demonstrated a significant main effect of time, $F_{3,95} = 291.0$; $p < 0.0001$, however, the main effect of peptide and the peptide by time interaction were not significant. Regression analysis showed that blood clearance of all four compounds can be described by biexponential functions. For all four peptides, the past component was extremely rapid ($t_{1/2} < 1$ min). The slow components were: P1; $t_{1/2} = 21.5 \pm 1.4$ min ($R^2 = 0.92$), P2; $t_{1/2} = 33.1 \pm 2.3$ min ($R^2 = 0.90$), P3; $t_{1/2} = 31.6 \pm 18$ min ($R^2 = 0.93$), P4; $t_{1/2} = 28.7 \pm 2.4$ min ($R^2 = 0.91$). For ^{111}In-labeled P1, the fraction of residual blood activity that was cell associated increased significantly with time ($p < 0.01$); 1 min: 40.9% ± 5.8%; 5 min: 41.6% ± 4.9%; 15 min: 45.5% ± 3.7%; 60 min: 51.5% ± 7.7%, and 90 min: 84.3% ± 4.3%, suggesting that white cell binding occurred immediately after injection and did not dissociate significantly during the interval of observation.

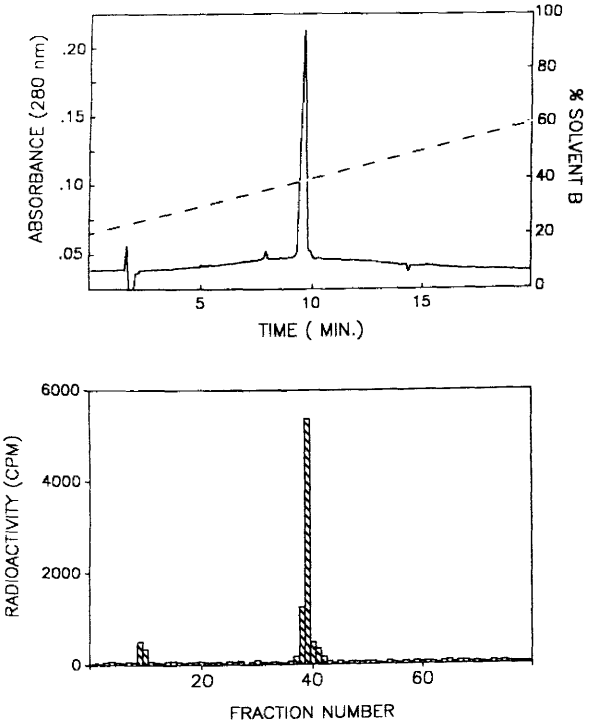

FIGURE 5
HPLC of ^{111}In-P1. The chromatogram was recorded after injection of a mixture of radiolabeled and unlabeled peptide. The upper panel corresponds to the UV absorption at 280 nm and the lower panel to radioactivity (CPM/fraction). The broken line in the upper panel illustrates the gradient.

Tissue accumulation (expressed as %ID/g) of all four ^{111}In-labeled chemotactic peptide analogs generally decreased with time (Table 1). In the heart, P2 and P3 had greater accumulation ($p < 0.01$) than P4 and P3 had greater accumulation than P1 ($p < 0.05$). In the lung, P1 and P2 had greater accumulation than P4 ($p < 0.01$ and $p < 0.05$). In the liver: P2 > P1 > P3 > P4 ($p < 0.01$). In the kidney, P1 had greater ($p < 0.01$) accumulation than P2, P3 and P4. In the spleen, P1 and P2 had greater ($p < 0.01$) accumulation than P3 and P4. In the gastrointestinal tract, P2 had greater ($p < 0.01$) accumulation than P1, P3, and P4. In muscle, P1 had greater ($p < 0.01$) accumulation than P2 and P4. In the testis, P1 had greater accumulation than P2, P3, and P4; P3 had greater accumulation than P4.

Infection Imaging

The animals tolerated the intravenous administration of the DTPA-derivatized chemotactic peptide analogs without apparent ill effects. All of the peptides had definite localization at the site of infection as early as 5 min after injection. Figure 7A shows gamma camera images of groups of rats acquired 5 min, 1, 1.5, and 2 hr after injection of 0.1 mCi of ^{111}In-P1. In the first

TABLE 1

Biodistribution of ^{111}In-Labeled Chemotactic Peptide Analogs (%ID/g, mean ± s.e.m.)

Organ	Time (min)	P1	P2	P3	P4
Heart	5	0.44 ± 0.05	0.48 ± 0.04	0.48 ± 0.04	0.45 ± 0.03
	30	0.17 ± 0.02	0.22 ± 0.008*	0.20 ± 0.04*	0.12 ± 0.007
	60	0.06 ± 0.006	0.08 ± 0.005	0.10 ± 0.02	0.05 ± 0.004
	120	0.02 ± 0.003	0.05 ± 0.005	0.05 ± 0.00	0.03 ± 0.002
Lung	5	1.09 ± 0.19*	1.02 ± 0.30*	0.67 ± 0.04	0.63 ± 0.09
	30	0.31 ± 0.03	0.32 ± 0.03	0.33 ± 0.02	0.17 ± 0.01
	60	0.14 ± 0.01	0.14 ± 0.02	0.18 ± 0.03	0.08 ± 0.006
	120	0.08 ± 0.009	0.12 ± 0.04	0.10 ± 0.01	0.05 ± 0.003
Liver	5	1.00 ± 0.05*	1.20 ± 0.10*	0.77 ± 0.05*	0.35 ± 0.02
	30	0.52 ± 0.03*	0.63 ± 0.03*†	0.45 ± 0.02*	0.15 ± 0.02
	60	0.53 ± 0.02*	0.48 ± 0.01*	0.41 ± 0.02*	0.09 ± 0.004
	120	0.40 ± 0.06*	0.47 ± 0.02*	0.41 ± 0.01*	0.08 ± 0.003
Kidney	5	9.45 ± 0.51*	3.81 ± 0.73*	5.40 ± 0.32*	4.13 ± 0.42*
	30	23.2 ± 1.10	3.38 ± 0.27	2.65 ± 0.53	2.73 ± 0.14
	60	22.3 ± 1.03	3.49 ± 0.68	2.55 ± 0.09	3.25 ± 0.67
	120	26.2 ± 1.28	3.06 ± 0.18	2.42 ± 0.12	3.31 ± 0.58
Spleen	5	0.36 ± 0.03*	0.37 ± 0.03*	0.21 ± 0.008	0.22 ± 0.01
	30	0.25 ± 0.04*	0.23 ± 0.02*	0.11 ± 0.005	0.14 ± 0.06
	60	0.21 ± 0.0*‡	0.13 ± 0.01‡	0.08 ± 0.004	0.04 ± 0.003
	120	0.15 ± 0.02	0.16 ± 0.03	0.07 ± 0.008	0.04 ± 0.003
GI tract	5	0.45 ± 0.03	0.51 ± 0.17‡	0.36 ± 0.02	0.35 ± 0.02
	30	0.18 ± 0.02	0.35 ± 0.08‡	0.20 ± 0.02	0.22 ± 0.09
	60	0.08 ± 0.008	0.25 ± 0.08‡	0.12 ± 0.01	0.06 ± 0.006
	120	0.04 ± 0.009	0.00 ± 0.00	0.10 ± 0.02	0.04 ± 0.006
Muscle	5	0.39 ± 0.03‡	0.31 ± 0.04	0.33 ± 0.02	0.33 ± 0.04
	30	0.14 ± 0.01‡	0.11 ± 0.01	0.13 ± 0.009	0.08 ± 0.007
	60	0.14 ± 0.06‡	0.06 ± 0.00	0.09 ± 0.008	0.04 ± 0.006
	120	0.02 ± 0.003	0.05 ± 0.00	0.03 ± 0.003	0.02 ± 0.002
Testicle	5	0.45 ± 0.02*	0.20 ± 0.04	0.27 ± 0.02‡	0.19 ± 0.06
	30	0.24 ± 0.02*‡	0.14 ± 0.02	0.17 ± 0.02	0.11 ± 0.004
	60	0.16 ± 0.02*	0.08 ± 0.006	0.07 ± 0.004	0.04 ± 0.004
	120	0.08 ± 0.02	0.05 ± 0.01	0.04 ± 0.002	0.02 ± 0.002

Each point is the mean ± s.e.m. for six animals. Heart: * $p < 0.01$; P2 and P3 vs. P4. Lung: * $p < 0.01$; P3 and P4 vs. P1 and P2. Liver: (5 min) * $p < 0.01$; P1 vs. P2 vs. P3 vs. P4, (30 min) * $p < 0.01$; P1, P2 and P3 vs. P4, † $p < 0.01$; P2 vs. P1, (60 min) * $p < 0.01$; P1, P2 and P3 vs. P4, (120 min) * $p < 0.01$; P1, P2 and P3 vs. P4. Kidney: * $p < 0.01$; P1 vs. P2, P3, and P4. Spleen: (5 and 30 min) * $p < 0.01$; P1 and P2 vs. P3 and P4, (60 min) ‡ $p < 0.05$; P1 vs. P2, P2 vs. P4, (120 min) ‡ $p < 0.05$; P1 and P2 vs. P3 and P4. Muscle: (5 min) ‡ $p < 0.05$; P1 vs. P2, (30 min) ‡ $p < 0.05$; P1 vs. P4, (60 min) ‡ $p < 0.05$; P3 vs. P2 and P4. Testis: (5 min) * $p < 0.01$; P1 vs. P2, P3 and P4, ‡ $p < 0.05$; P3 vs. P2, (30 min). * $p < 0.01$; P1 vs. P4, * $p < 0.05$; P1 vs. P2, (60 min) * $p < 0.01$; P1 vs. P3 and P4, * $p < 0.05$; P1 vs. P2.

image, there was a slight suggestion of lesion localization. Accumulation of radionuclide (target-to-background ratio) was maximal at 1 hr after injection and decreased in the later images. In addition to the lesion, radionuclide also accumulated in the kidneys. There was no evidence of significant radionuclide accumulation in the liver, spleen, bone or gastrointestinal tract. To evaluate the effect of increased permeability of infected tissue on peptide accumulation, ^{111}In-P1 and ^{99m}Tc-DTPA (a marker of extracellular space) were co-injected in another group of animals and simultaneous images were acquired (data not shown). In these experiments, the images acquired in the ^{99m}Tc window were of lower intensity and decreased in intensity more rapidly than those acquired in the ^{111}In window (upper peak). Figure 7B shows gamma camera images of groups of rats acquired at 5, 15, 30, and 60 min after injection of 0.1 mCi of ^{111}In-P4. With this peptide, maximal radionuclide accumulation was detected in the 30-min image and there was a slight decrease in image quality in the later images. The extra-lesion distribution of radionuclide in these images was similar to that observed with ^{111}In-P1. Similar patterns of normal organ and lesion accumulation of radioactivity was seen with the other two peptides.

T/B ratios and %RA as a function of time after injection for the different peptides are shown in Figure 8. Analysis of variance of the T/B data showed a significant main effect of time after injection, $F_{3,75} = 74.51$; $p < 0.0001$. At 15 and 30 min, T/B was greater than at 5 min but less than at 60 min ($p < 0.01$). The individual peptides did not show statistically significant

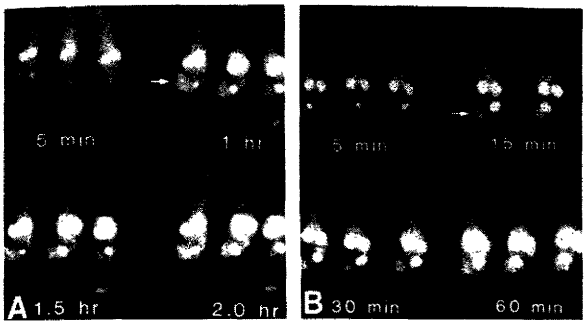

FIGURE 7
Serial gamma camera images of rats with *E. coli* deep-thigh infections, after injection of ^{111}In-labeled chemotactic peptide analogs. (A) Images of groups of rats acquired 5 min, 1, 1.5, and 2 hr after injection of 0.1 mCi of ^{111}In-P1. (B) Images of groups of rats acquired at 5, 15, 30, and 60 min after injection of 0.1 mCi of ^{111}In-P4. At 15 min, only two animals were imaged. For all animals, infections were produced 24 hr prior to injection.

differences in T/B ratio ($p > 0.1$). Also, peptide by time interaction was not significant ($p > 0.5$). For %RA, analysis of variance showed a significant main effect of time after injection, $F_{3,75} = 3.47$; $p < 0.005$. At 60 min, %RA was significantly lower than at 5, 15, or 30 min. The individual peptides did not show statistically significant differences in %RA ($p > 0.2$). Also, peptide by time interaction was not significant ($p > 0.99$).

DISCUSSION

The results of this study demonstrate that ^{111}In-labeled chemotactic peptide analogs are effective agents for the external imaging of focal sites of infection in an experimental model of deep-thigh infection. Since the first report of the chemoattractant properties of small N-formyl peptides (*7*), these compounds have attracted increasing attention (*23*). Numerous structure-activity studies directed at determining the particular features of this molecule that are responsible for its many different biologic activities have been performed (6,24–26). Most of these studies have concentrated on amino acid substitutions in the ForMLF sequence. There have, however, been some reports of the synthesis and biologic activity of extended peptides (*27*). In fact, one of the most potent analogs reported is the hexapeptide, ForNleLFNleYK. In general, the results of the structure-activity studies have established that while modification of the N-terminous has profound effects on biologic activity, C-terminal changes have minimal effects (*28*). To date, there have been no studies on the effect of net charge on bioactivity.

In the present study, we prepared a series of chemotactic peptides with the C-terminus extended with a DTPA-derivatized Lys, Lys(NH_2), or a diamino group. These modifications result in molecules of net charges −4 to −5, and compared to −1 for ForMLF. The synthetic peptides were of high chemical purity, were

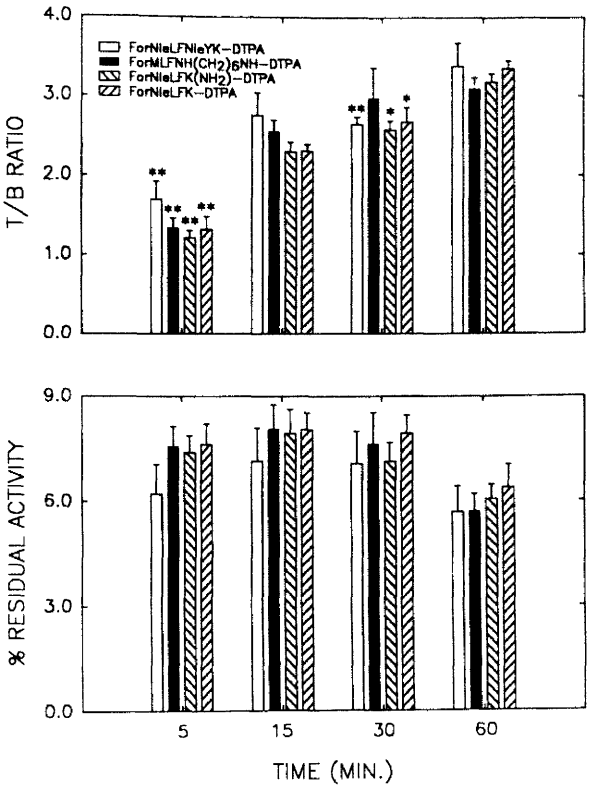

FIGURE 8
T/B ratio and % RA of sites of infection in rats with *E. coli* deep-thigh infections imaged at 5, 15, 30, and 60 min after injection of ^{111}In labeled chemotactic peptide analogs. In all cases, infections were established 24 hr prior to injection. Each point is the mean ± s.e.m. for 5–6 animals. *$p < 0.05$, **$p < 0.01$. ForNleLFNleYK-DTPA: P1, ForMLFNH(CH_2)$_6$NH-DTPA: P2, ForNleLFK(NH_2)-DTPA: P3, ForNleLFK-DTPA: P4.

readily labeled with ^{111}In (Fig. 5), maintained biologic activity (Fig. 1), and had affinities for the oligopeptide chemoattractant receptors on human neutrophil that were similar to or greater than the native tripeptide (Fig. 2). In addition, as has been previously reported for other chemotactic peptide analogs (*6,8*), the biologic activity of these molecules was closely correlated with receptor binding (Fig. 3). The high affinity of these peptides is consistent with the previously proposed conformation for the ligand receptor complex in which only the N-terminal amino acid residues of the peptide interact with the receptor (*29*).

In addition to having high affinity for WBC receptors in vitro, this activity appears to persist in vivo as demonstrated by the cell association of the radiolabel and the images of infection in the rat. While these results suggest that the mechanism of infection localization may be due to binding to phagocytes, this has not as yet been conclusively proven. The rapid localization (within 1 hr) of radiolabeled chemotactic peptide analogs at sites of experimental infection has clear advantages over other radionuclide methods for infection localization. Gallium-67-citrate, ^{111}In-labeled WBCs,

and ^{111}In-labeled IgG typically require more than 6 hr between injection and imaging and are thus not useful for evaluating acute processes such as appendicitis for which there is currently no effective imaging procedure. In addition, the observation that the peptide-based imaging agents have much lower levels of accumulation in background organs (except for the kidney) than the other agents adds to their potential superiority. Another advantage of the radiolabeled peptides is an early decrease in image intensity. This property makes the agents potentially useful for monitoring response to therapy, since, repetitive injections and imaging should not be confounded by residual activity from earlier studies. The mechanism for the rapid clearance of activity from lesion sites has not as yet been investigated. However in vitro studies with ^{125}I-labeled chemotactic peptide analogs, have demonstrated that peptide-receptor complexes are internalized and degraded by PMNs with release of the radiolabel (*11*). It is unlikely that this can explain the rapid decrease in lesion radioactivity after injection of ^{111}In-labeled peptides, since previous studies have shown that following internalization of ^{111}In-labeled proteins the label is retained in the cell.

Other investigators have explored the possibility of using radiolabeled chemotactic peptides for leukocyte labeling (*30–32*). Unfortunately, the radiolabeling methods available at the time of these studies yielded agents of relatively low specific activity and required pharmacologic amounts of peptide for imaging. These doses of peptide were shown to produce profound transient neutropenia in rabbits (*33*). Similar doses of the synthetic peptides evaluated in the current study also produced neutropenia in rabbits (data not shown). The implications of this neutropenia in rabbits for human imaging is not clear, however, since peripheral white counts decreased minimally in rats (Fig. 4). While pharmacologic doses of peptide were used in the imaging studies reported here, we have recently demonstrated that 10-fold lower amounts of peptide can be labeled to the same level of radioactivity with ^{111}In. In addition, because of the short biologic half-time of the peptides, ^{111}In is not the radionuclide of choice for imaging. If the compounds can be labeled with ^{99m}Tc, even higher specific activities should be obtainable. Also ^{11}C, ^{68}Ga, or ^{18}F-labeling of the peptides should be feasible, making possible the use of such reagents for positron emission tomography. Currently, these alternate labeling techniques are under investigation in our laboratory. Regardless of the radiolabel that ultimately proves to be optimal for radionuclide imaging with chemotactic peptide analogs, it is clear that additional studies in other species (including primates) will be required before the agents can be evaluated in human subjects.

In conclusion, the results of this study establish that radiolabeled chemotactic peptide analogs are effective agents for imaging focal sites of infection. The potential advantages of these molecules over currently available methods of localizing lesions are numerous and clearly justify further investigation.

ACKNOWLEDGMENTS

This work was supported in part by grants from the R.W. Johnson Pharmaceutical Research Institute, the Edw. Mallinkrodt, Jr. Foundation, Shriners Burn Institute grant 15876 and Department of Energy grant DE-FG02-86ER60460.

REFERENCES

1. McNeil BJ, Sanders R, Alderson PO, et al. A prospective study of computed tomography, ultrasound, and gallium imaging in patients with fever. *Radiology* 1981;139:647–653.
2. Froelich JW, Swanson D. Imaging of inflammatory processes with labeled cells. *Semin Nucl Med* 1984;14:128–140.
3. Fischman AJ, Rubin RH, Khaw BA, et al. Detection of acute inflammation with ^{111}In-labeled non-specific polyclonal IgG. *Semin Nucl Med* 1988;18:335–344.
4. Rubin RH, Fischman AJ, Callahan RJ, et al. ^{111}In-labeled nonspecific immunoglobulin scanning in the detection of focal infection. *N Engl J Med* 1989;321:935–940.
5. Tzen KY, Oster ZH, Wagner HN, Tsan MF. Role of iron-binding proteins and enhanced vascular permeability in the accumulation of gallium-67. *J Nucl Med* 1980;21:31–35.
6. Showell HJ, Freer JR, Zigmond SH, et al. The structural relations of synthetic peptides as chemotactic factors and inducers of lysosomal enzyme secretion for neutrophils. *J Exper Med* 1976;143:1154–1169.
7. Schiffmann E, Corcoran BA, Wahl SM. Formylmethionyl peptides as chemoattractants for leukocytes. *Proc Natl Acad Sci USA* 1975;72:1059–1062.
8. Williams LT, Snyderman R, Pike MC, Lefkowitz RJ. Specific receptor sites for chemotactic peptides on human polymorphonuclear leukocytes. *Proc Nat Acad Sci USA* 1977;74:1204–1208.
9. Snyderman R, Verghese MW. Leukocyte activation by chemoattractant receptors: role of a guanine nucleotide regulatory protein and polyphosphoinositide metabolism. *Rev Infect Dis* 1987;9:S562–S569.
10. Fletcher MP, Seligman BE, Gallin JI. Correlation of human neutrophil secretion, chemoattractant receptor mobilization, and enhanced functional capacity. *J Immunol* 1988;128:941–948.
11. Niedel J, Wilkinson S, Cuatrecasas P. Receptor mediated uptake and degradation of ^{125}I-chemotactic peptide by human neutrophils. *J Biol Chem* 1979;10:700–710.
12. Niedel J, Davis J, Cuatrecasas P. Covalent affinity labeling of the formyl peptide chemotactic receptor. *J Biol Chem* 1980;255:7063–7066.
13. Merrifield RB. Solid phase peptide synthesis. I. Synthesis of a tetrapeptide. *J Am Chem Soc* 1963;15:2149–2154.
14. Stewart JM, Young JD. *Solid-phase peptide synthesis.* San Francisco. W.H. Freeman & Company; 1969.
15. Gisin BF. Preparation of Merrifield-resins through total esterification with cesium salts. *Helv Chim Acta* 1973;56:1476–1482.
16. Sheehan JC, Yang DDH. The use of N-formylamino acids in peptide synthesis. *J Am Chem Soc* 1958;80:1154–1160.
17. DeGrado WF, Kaiser ET. Polymer-bound oxime esters as supports for solid phase peptide synthesis-preparation of protected peptide fragments. *J Org Chem* 1980;45:1295–1300.

18. Boyum A. Isolation of mononuclear cells and granulocytes from human blood: isolation of mononuclear cells by one centrifugation and granulocytes by combining centrifugation and sedimentation at 1 g. *Scand J Clin Lab Invest* 1968;21:77–89.
19. Pike MC, Snyderman R. Leukocyte chemoattractant receptors. *Methods Enzymol* 1988;162:236–245.
20. Pike MC, Jakoi L, McPhail LC, Snyderman R. Chemoattractant-mediated stimulation of the respiratory burst in human polymorphonuclear leukocytes may require appearance of protein kinase activity in the cell's particulate fraction. *Blood* 1986;67:909–913.
21. Baker HC, Lindsey RJ, Weisbroth SH. *The laboratory rat.* New York: Academic Press; 1980:257.
22. Duncan DB. Multiple range tests and multiple F-tests. *Biometrics* 1955;11:1–42.
23. Becker EJ. The formylpeptide receptor of the neutrophil a search and conserve operation. *Am J Pathol* 1987;129:16–24.
24. O'Flaherty JT, Showell HJ, Kreutzer DL, Ward PA, Becker EL. Inhibition of in vivo and in vitro neutrophil responses to chemotactic factors by a competitive antagonist. *J Immunol* 1978;120:1326–1332.
25. Rot A, Henderson LE, Copeland TD, Leonard EJ. A series of six ligands for the human formyl peptide receptor: tetrapeptides with high chemotactic potency and efficacy. *Proc Natl Acad Sci USA* 1987;84:7967–7971.
26. Iqbal M, Balaram P, Showell HJ, Freer RJ, Becker EL. Conformationally constrained chemotactic peptide analogs of high biological activity. *FEBS* 1984;165:171–174.
27. Toniolo C, Bonora GM, Showell H, Freer RJ, Becker EL. Structural requirements for formyl homooligopeptide chemoattractants. *Biochem* 1984;23:698–704.
28. Spisani S, Cavalletti T, Gavioli R, Scatturin A, Vertuani G, Traniello S. Response of human neutrophils to formyl-peptide modified at the terminal amino and carboxyl groups. *Inflammation* 1986;10:363–369.
29. Freer RJ, Day AR, Muthukumaraswamy N, Pinon D, Showell HJ, Becker EL. Formyl peptide chemoattractants: a model of the receptor in rabbit neutrophils. *Biochem* 1982;21:257–263.
30. McAfee JG, Subramanian G, Gagne G. Techniques of leukocyte harvesting and labeling: problems and perspectives. *Semin Nucl Med* 1984;14:83–106.
31. Thakur ML, Seifer CL, Madsen MT, McKenney SM, Desai AG, Park CH. Neutrophil labeling: problems and pitfalls. *Semin Nucl Med* 1984;14:107–117.
32. Zogbhi SS, Thakur ML, Gottschalk A, et al. A potential radioactive agent for labeling of human neutrophils [Abstract]. *J Nucl Med* 1981;22:P32.
33. O'Flaherty JT, Showell HJ, Ward PA. Neutropenia induced by systemic injection of chemotactic factors. *J Immunol* 1977;118:1586–1589.

EDITORIAL
Chemotactic Peptides: New Locomotion for Imaging of Infection?

Approximately one year ago, Fischman, Khaw, and Strauss expressed their disappointment about the relatively slow progress with radioimmune imaging in neoplasia, while success in non-neoplastic areas had been very encouraging (*1*). Among other molecules, which do not directly involve the immune response, leukocyte-attractant peptides, which were originally derived from bacteria, were proposed as agents for imaging the cells to which they bind. The authors noted three potential advantages of this type of molecule over antibodies: smaller size and hence better diffusibility to the extravascular space; faster blood clearance resulting in low background activity; and the presence of well-defined receptor systems on known populations of tissue cells. Furthermore, analogs of these peptides can be synthesized and, by varying the size, charge, and other properties, a radiopharmaceutical with optimal imaging characteristics can be selected.

In this issue, Fischman et al. (*2*) report their study using such labeled chemotactic peptide analogs to image focal sites of infection. The study was performed in rats with a deep-thigh infection caused by *Escherichia coli*. Four different analogs were synthesized, coupled to diethylenetriaminepentaacetic acid (DTPA) and labeled with indium-111 (^{111}In). The parent compound of the molecules, N-formyl-methionyl-leucyl-phenylalanine (N-formyl-Met-Leu-Phe) has a molecular weight of 437. Five minutes after injection in rats, definite localization of the ^{111}In-labeled DTPA-derivatized chemotactic peptide analogs was present at the site of infection, thus showing rapid diffusion to the extravascular space. To evaluate the effect of increased permeability of infected tissue on peptide accumulation, a group of animals was co-injected with ^{99m}Tc-DTPA and ^{111}In-labeled DTPA-derivatized chemotactic peptide analogs. The authors reported that the images acquired in the ^{99m}Tc-window were of lower intensity and decreased in intensity more rapidly than those acquired in the ^{111}In-window using the upper peak only. One might wonder whether this is a fair comparison since both compounds differ significantly in molecular size, radiolabel, charge, renal handling, and other characteristics that are known to influence local accumulation and wash-out in regions with increased permeability such as infected tissue. To better understand the impact of molecular size and other properties, further experiments are needed.

Received Dec. 7, 1990; accepted Dec. 7, 1990
For reprints contact: Frans H.M. Corstens, MD, Department of Nuclear Medicine, University Hospital Nijmegen, P.O. Box 9101, 6500 HB Nijmegen, The Netherlands.